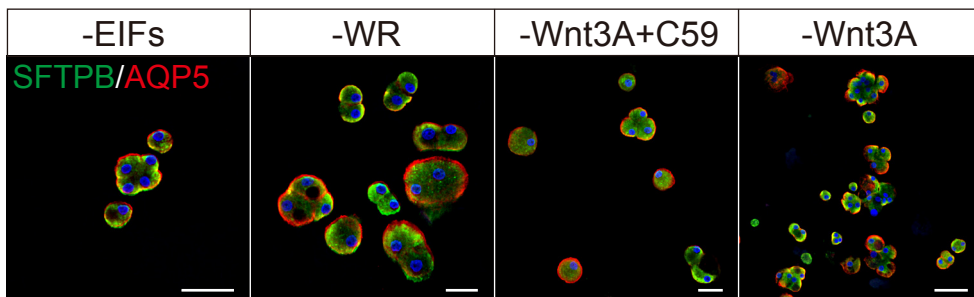


Supplemental information

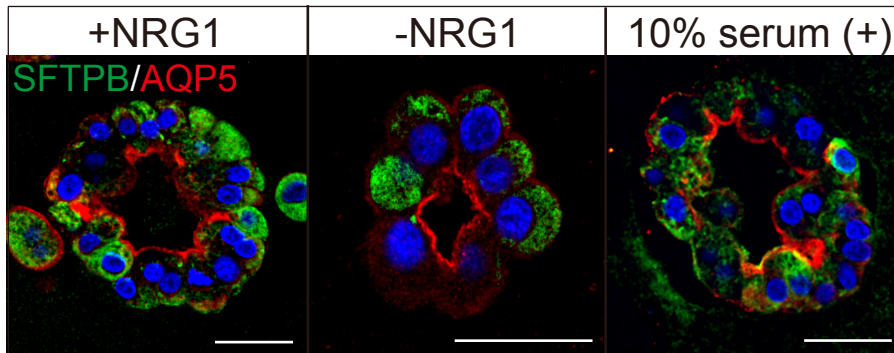
**Direct derivation of human alveolospheres
for SARS-CoV-2 infection modeling
and drug screening**

Toshiki Ebisudani, Shinya Sugimoto, Kei Haga, Akifumi Mitsuishi, Reiko Takai-Todaka, Masayuki Fujii, Kohta Toshimitsu, Junko Hamamoto, Kai Sugihara, Tomoyuki Hishida, Hisao Asamura, Koichi Fukunaga, Hiroyuki Yasuda, Kazuhiko Katayama, and Toshiro Sato

A



B



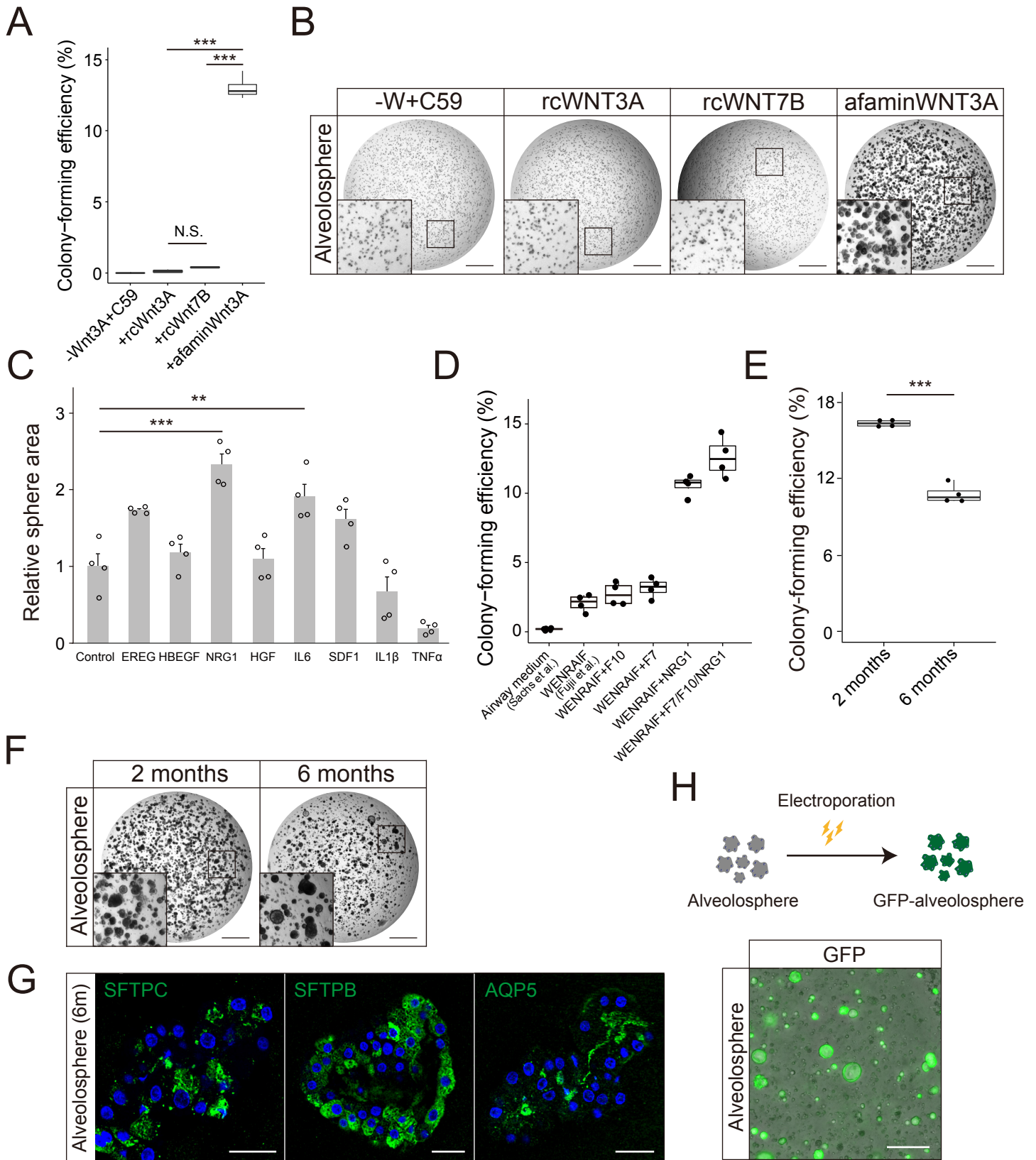


Figure S2

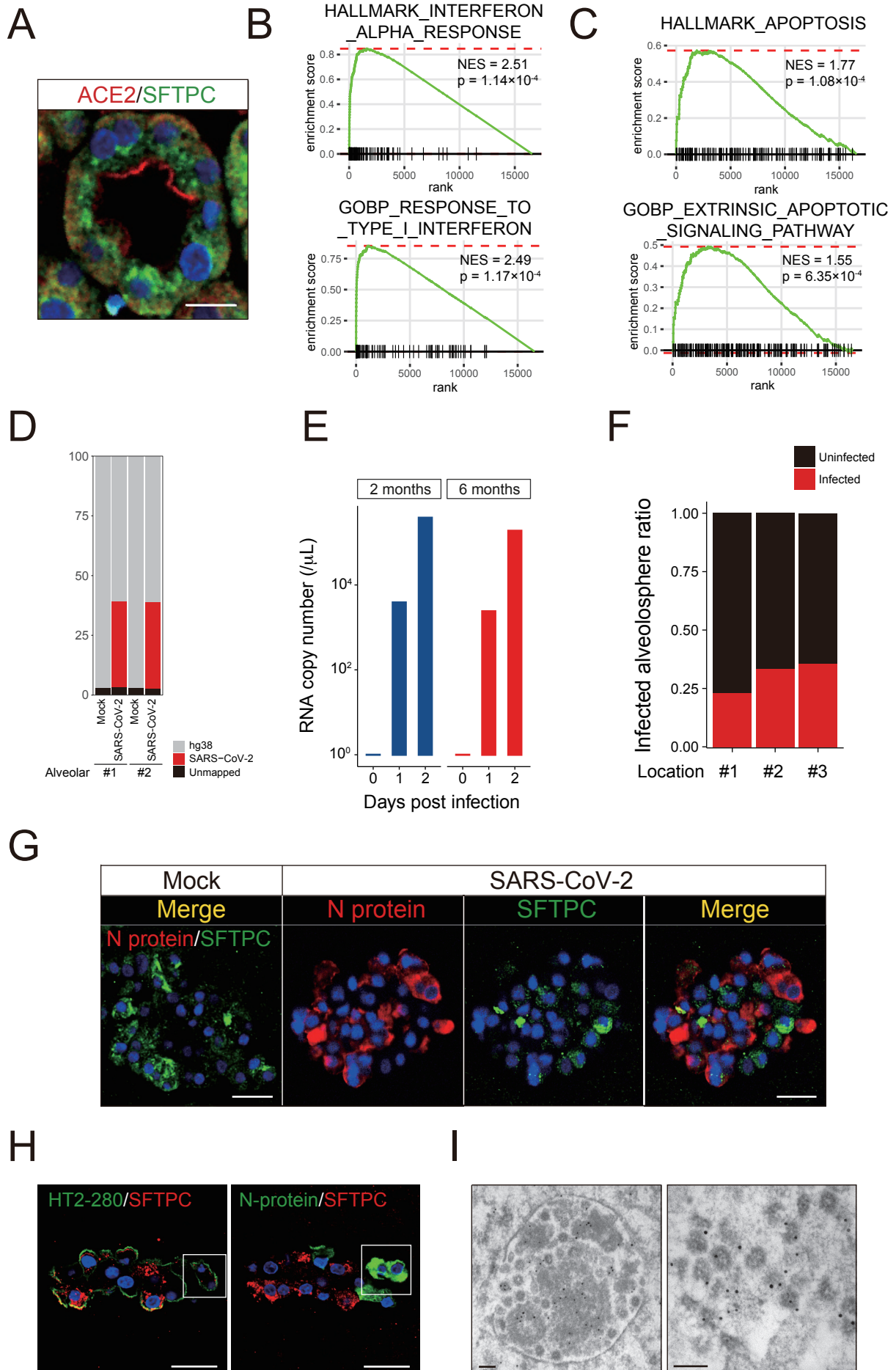


Figure S3

Figure S1. Immunostaining of Human Alveolospheres, Related to Figure 1.

(A) Co-staining of SFTPB (green) and AQP5 (red) in alveolospheres cultured with -EIFs, -WR, -Wnt3A+C59 or -Wnt3A. (B) Co-staining of SFTPB (green) and AQP5 (red) in alveolospheres cultured with WENRAIFs and NRG1 (+NRG1, left), WENRAIFs (-NRG1, middle) or WENRAIFs with 10% serum (right). Nuclear counterstaining, Hoechst 33342 (F, G). Scale bar: 2 μ m (D, right), 10 μ m (D, left), 25 μ m (E, right, F, G), and 100 μ m (E, left).

Figure S2. Long-term Efficient Expansion of Alveolospheres, Related to Figure 2.

(A) Colony-forming efficiency of C59-treated alveolospheres (passage 14) in the presence of recombinant Wnt3A (300 ng/mL), recombinant Wnt7B (300 ng/mL) and afamin-Wnt3A or absence of Wnt. Data are demonstrated as mean \pm SEM. ***P < 0.001, Welch's unpaired t-test. N.S., not significant. rc, recombinant. (B) Representative bright-field images of alveolospheres expanded from single cells cultured with ENRAIFs + C59 with recombinant Wnt3A, recombinant Wnt7B and afamin-Wnt3A or without Wnt. 5,000 cells were plated per well. (C) The effect of various growth factors and cytokines on the growth of a human alveolosphere line (passage 8). The sphere area was measured on day 21 post plating. Dots show the area of alveolospheres in each well relative to the control. Data are demonstrated as mean \pm SEM. (D) Colony-forming efficiency of alveolospheres (passage 5) in airway medium (Sachs et al., 2019), intestinal medium (IM) (Fujii et al., 2018), IM with FGF-10 (F10), FGF-7 (F7) or NRG1, and WENARIFs (this study). Data are demonstrated as mean \pm SEM. (E) Colony-forming efficiency of early- (2 months) and late-passaged (6 months) alveolospheres. Data are demonstrated as mean \pm SEM. ***P < 0.001, Welch's unpaired t-test. (F) Representative bright-field images of early- (2 months) and late-passaged (6 months) alveolospheres. (G) Immunostaining of SFTPC (green, left), SFTPB (green, middle) and AQP5 (green, right) in late-passaged (6 months) alveolospheres. (H) Successful GFP-labeling of alveolospheres by electroporation (passage 1, day 11). Nuclear counterstaining, Hoechst 33342 (G). Inset shows higher magnification. Scale bar, 25 μ m (G), 1 mm (B, F, H). **P < 0.01, ***P < 0.001, Welch's unpaired t-test.

Figure S3. Characterization of SARS-CoV-2-infected Human Alveolospheres, Related to Figure 3.

(A) Co-staining of SFTPC (green) and ACE2 (red) in alveolospheres. (B) Enrichment of two independent interferon-related gene sets in SARS-CoV-2-infected versus mock-infected alveolospheres. NES, normalized enrichment score. (C) Enrichment of two independent apoptosis-related gene sets in SARS-CoV-2-infected versus mock-infected alveolospheres. (D) Percentage of SARS-CoV-2 RNA reads in alveolospheres transcriptomes. Two independent experiments are shown (#1; passage 6, #2; passage 4). (E) Analysis of the SARS-CoV-2 RNA copy number in the culture medium of 2 month or 6 month-old alveolospheres following infection (MOI = 5). Copy numbers are shown as RNA copies per 1 μ L of the culture medium. (F) Proportion of alveolospheres (passage 7) infected with SARS-CoV-2 at 2 dpi (MOI = 5). (G) Co-staining of SARS-CoV-2 nucleocapsid (N) protein (red) and SFTPC (green) in mock-infected

(left) or SARS-CoV-2-infected (right) alveolospheres (passage 5) (MOI = 5). (H) Co-staining of HT2-280 (green) and SFTPC (red) (left), and N protein (green) and SFTPC (red) (right). (I) Immuno-gold staining of spike protein of SARS-CoV-2 in infected alveolospheres (passage 5) (MOI = 5). Scale bar, 50 nm (I), 10 μm (A), and 25 μm (G, H). Nuclear counterstaining, Hoechst 33342 (A, G, H).

Table S1. Reagents for Alveolosphere Culture, Related to STAR Methods.

Reagent name	Supplier	Cat No.	Final concentration
Matrigel, Growth factor reduced	BD Biosciences	Cat#356231	-
Advanced DMEM/F12	Thermo Fisher Scientific	Cat#12634010	-
HEPES	Thermo Fisher Scientific	Cat#15630080	100× diluted
GlutaMAX Supplement	Thermo Fisher Scientific	Cat#35050061	100× diluted
Penicillin-Streptomycin	Thermo Fisher Scientific	Cat#15140122	100/100 U/mL
B-27 Supplement	Thermo Fisher Scientific	Cat#17504044	50× diluted
N-Acetyl-L-cysteine	Sigma-Aldrich	Cat#A9165	1 mM
[Leu ¹⁵]-Gastrin I human	Sigma-Aldrich	Cat#G9145	10 nM
Afamin-Wnt-3A serum-free conditioned medium	Mihara et al., 2016	N/A	25% v/v
Recombinant mouse EGF	Thermo Fisher Scientific	Cat#PMG8043	50 ng/mL
Recombinant human IGF-1	BioLegend	Cat#590904	100 ng/mL
Recombinant human FGF-basic	Peprotech	Cat#100-18B	50 ng/mL
Recombinant human FGF-10	Peprotech	Cat#100-26	100 ng/mL
Recombinant human KGF (FGF-7)	Peprotech	Cat#100-19	5 ng/mL
Recombinant human neuregulin-1 (Heregulin β -1)	Peprotech	Cat#100-03	100 ng/mL
Recombinant mouse Noggin	Peprotech	Cat#250-38	100 ng/mL
R-spondin-1 conditioned medium	Ootani et al., 2009	N/A	10%
A83-01	Tocris	Cat#2939	500 nM
Y-27632	FUJIFILM Wako Pure Chemical	Cat#253-00513	10 μ M

Table S2. Patient Characteristics, Related to STAR Methods.

Patient	Cell type	Age	Gender	Brinkman index	Expansion duration	Background disease
1	Alveolar	75	M	1000	>8 months	Lung cancer
2	Alveolar	54	F	0	>8 months	Lung cancer
3	Alveolar	47	F	0	>6 months	Lung cancer
4	Alveolar	70	M	0	>6 months	Metastatic colorectal cancer
5	Alveolar	76	M	500	>6 months	Lung cancer
6	Alveolar	74	F	0	>6 months	Lung cancer
7	Alveolar	80	F	0	>5 months	Lung cancer
8	Alveolar	63	M	480	>4 months	Lung cancer
9	Alveolar	69	M	0	>4 months	Hamartoma
10	Airway	75	M	800	>8 months	Lung cancer
11	Airway	85	M	0	>6 months	Lung cancer

Gender; M: male, F: female